

Temporal Decomposition for Improved Unit Commitment in Power System Production Cost Modeling

Kibaek Kim, *Member, IEEE*, Audun Botterud, *Member, IEEE*, and Feng Qiu, *Senior Member, IEEE*

Abstract—Long-term planning in power systems requires simulations of unit commitment (UC) for long time periods up to 20 years. Such simulations are conducted with production cost models (PCMs), which involve solving large-scale mixed-integer programming (MIP) problems with a large number of variables and constraints, because of the long planning horizon. We have developed new optimization modeling and solution techniques based on a decomposition scheme to reduce the solution time and improve the accuracy in PCMs. We propose a temporal decomposition that solves the UC problem by systematically decoupling the long-horizon MIP problem into several subhorizon models. The decomposition is obtained by the Lagrangian relaxation of the time-coupling constraints such as ramping constraints and minimum uptime/downtime constraints. The key challenge is to solve several sub-MIP problems while effectively searching for dual variables to accelerate the convergence of the algorithm. We implement the temporal decomposition in an open-source parallel decomposition framework, which can solve the multiple subproblems in parallel on high-performance computing clusters. We also implement the branch-and-bound method on top of the decomposition in order to find a primal optimal solution. Numerical results of the decomposition method are reported for the IEEE 118-bus and PEGASE 1354-bus test systems with up to an 168-hour time horizon.

Index Terms—Production cost model, mixed-integer programming, decomposition method, parallel computing

NOMENCLATURE

Sets:

\mathcal{G}	Generators
\mathcal{G}_n	Generators at bus n
\mathcal{K}	Generation cost blocks
\mathcal{L}	Transmission lines
\mathcal{L}_n^+	Transmission lines to bus n
\mathcal{L}_n^-	Transmission lines from bus n
\mathcal{N}	Buses
\mathcal{T}	Time periods, $= \{1, \dots, T\}$, where T is the number of periods.

Parameters:

B_l	Susceptance of transmission line l
C_{gk}	Generation cost of generator g for generation cost block k
D_{nt}	Demand load of bus n at time t

K. Kim is with the Mathematics and Computer Science Division at Argonne National Laboratory, Lemont, IL 60439 and also with the Computation Institute, University of Chicago, Chicago, IL 60637 USA.

A. Botterud and F. Qiu are with the Energy Systems Division at Argonne National Laboratory, Lemont, IL 60439.

Manuscript received XXX; revised XXX.

DT_g	Minimum downtime of generator g
F_l	Power capacity of transmission line l
P_g^{max}	Maximum power generation of generator g
P_g^{min}	Minimum power generation of generator g
R_g^+	Ramp-up capacity of generator g
R_g^-	Ramp-down capacity of generator g
S_g	Startup cost of generator g
K_g	Commitment cost of generator g
UT_g	Minimum uptime of generator g
γ^+	Spinning-up reserve requirement
γ^-	Spinning-down reserve requirement
Θ_n^{min}	Minimum phase-angle of bus n
Θ_n^{max}	Maximum phase-angle of bus n
Variables:	
f_{lt}	Power flow in transmission line l at time t
p_{gt}	Power generation from generator g at time t
s_{gkt}	Power generation from generator g at price block k at time t
r_{gt}^+	Reserve-up generation of generator g at time t
r_{gt}^-	Reserve-down generation of generator g at time t
u_{gt}	Commitment of generator g at time t
v_{gt}	Startup of generator g at time t
θ_{nt}	Phase-angle of bus n at time t

I. INTRODUCTION

Production cost models (PCMs) are a class of computational tools that simulate power system operations over an extended (multimonth or multiyear) time horizon. The models leverage optimization techniques to compute unit commitment (UC) and economic dispatch (ED) schedules for a power system. PCMs are the dominant approach to performing cost-benefit analyses in the electricity grid industry. System operators, utilities, generation companies, regulators, and policy analysts use PCMs for long-term planning purposes, analyzing the impacts of potential future configurations of the power system. For instance, PCMs are frequently used in renewable integration studies (e.g. [1]). However, as the power system evolves in terms of scale (e.g., the growing size of independent system operators) and structure (e.g., rapidly increasing renewables penetration rates [2], the introduction of smart grid technologies [3]), current PCMs are not adequately addressing the requirements with respect to the future power grid. For example, model resolution is currently sacrificed in order to obtain tractable run times, and improved algorithms are needed to better capture the impact of the uncertainty associated

with renewables. Consequently, PCMs increasingly do not reflect the evolving grid reality and consequently impact the accuracy of cost-benefit analyses that decision makers use to guide investment, regulations, and policy in the electric power industry.

The major challenge that hinders high-fidelity, multisenario PCM simulation is computational tractability. In a realistic PCM simulation performed by system operators, the system may consist of several hundreds to thousands of buses and hundreds of generators. The PCM simulations could extend the individual UC optimization problem for multiple weeks. For a real system with a multiyear simulation period, weekly optimization horizon for the underlying UC problems, and hourly time resolution, the computational time is often impractical, especially when multiple scenarios are to be evaluated.

A number of researchers have proposed approaches to reduce the computational burden, such as a rolling horizon approach [4], time-domain partitioning [5], and various decomposition and inexact approximations (e.g., [6]–[9]). A rolling-horizon approach has been used in many studies (e.g., [4]). Although this approach reflects the daily operational practice in electricity markets, it only provides a suboptimal solution to the UC problem for a given planning horizon. Benders decomposition, as used in [6] cannot be applied to our problem since the integer variables appeared in the subproblems. If the integer restrictions are relaxed, significant optimality gaps occur, as shown in [10]. The approaches used in [7]–[9] are also based on the Lagrangian relaxation, which provides lower and upper bounds due to duality gap.

In essence, most PCMs today end up solving a number of deterministic multi-day/week UC optimization problems in sequence, and this is where most of the computational effort is required. The UC problem is a fundamental part of power system planning and operation and is also a notoriously hard problem to solve from an optimization perspective, given the binary decision variables and inter-temporal constraints involved. An extensive body of research has gone into improved solutions for the deterministic UC problem [11]. More recently, triggered by the influx of renewable energy, stochastic UC formulations have also received extensive attention in the research domain [12].

To increase the computational performance and accuracy of PCM simulations, we focus on solving the deterministic UC problem more efficiently by decomposing it into smaller time periods. The method, called *temporal decomposition*, is obtained by the Lagrangian relaxation of time-coupling constraints such as ramping capacities and minimum up/down time limits in the long-term UC problem. The key challenge with this decomposition approach is to solve several mixed-integer programming (MIP) problems while effectively searching for dual variables in order to accelerate the convergence of the algorithm. We develop a branch-and-bound method based on temporal decomposition that can solve multiple subproblems in parallel on high-performance computing (HPC) clusters. The method guarantees an optimal solution for the long-term UC problem.

The Lagrangian relaxation was first applied in [13] and has been an effective approach to UC problems in different

forms for more than two decades (e.g., [7], [14], [15]). In particular, a Lagrangian relaxation, similar to our temporal decomposition, has been applied in [7], where a long-term UC problem is decomposed into shorter-term UC problems by relaxing the time-coupling constraints for fuel and emission limits. However, the other coupling constraints, such as the ramping and minimum up/down time constraints, were ignored. Consequently, the decomposition approach in [7] provides only suboptimal solutions with unknown gaps.

A key task for an efficient Lagrangian relaxation method is finding good Lagrangian multipliers. Different methods have been developed for solving Lagrangian dual problems (e.g., [16]). We use a proximal bundle method in order to find the best Lagrangian dual bound. The proximal bundle method is a variant of the bundle method that outer-approximates the Lagrangian dual function by adding a set of linearly inequalities, with a proximal term in the objective function. Each iteration of the proximal bundle method either finds new dual multipliers for the subproblems or certifies the best Lagrangian dual bound.

However, such a Lagrangian relaxation method, also called *dual decomposition* (DD), suffers from the lack of primal solution characterization and the inability to recover primal feasible solutions. To overcome issues, we additionally solve the dual of the Lagrangian dual problem for given linear inequalities generated from the DD. Note that this can be seen as Dantzig-Wolfe decomposition with column generation [17]. This provides the primal characterization of solutions that can be used to guarantee integer feasibility by a branching procedure in the branch-and-bound method.

The contributions of this paper are summarized as follows.

- 1) Developing a novel parallel temporal decomposition based on the combination of branch-and-bound with Lagrangian relaxation of the time-coupling constraints to generate optimal solutions of the UC problem.
- 2) Implementing the parallel temporal decomposition (i.e., the combination of branch-and-bound with Lagrangian relaxation) in an open-source software package DSP, which enables effective computation on either desktop computer or HPC cluster.
- 3) Providing computational results on two test systems, indicating potential for substantial reductions in solution time.

We note that the proposed decomposition scheme has potential applications in market and system operations, not only in PCM planning studies.

The rest of the paper is organized as follows. In Section II we present a MIP formulation for the UC problem considered in this paper. Section III presents the temporal decomposition that decouples the UC problem into shorter-time subproblems. We also present the dual and Dantzig-Wolfe decompositions of the problem, followed by the branch-and-price method based on the decomposition schemes. In Section IV we show computational results from the temporal decomposition for solving the long-term UC problem on the IEEE 118-bus and PEGASE 1354-bus test systems. The conclusions of this paper are discussed in Section V.

II. UNIT COMMITMENT MODEL FOR PRODUCTION COST MODEL

In this section we present a UC model formulation that is solved in a PCM simulation for an extended time horizon. The UC model is formulated as a MIP problem [18] (also see [19] for major UC formulations),

$$\min \sum_{g \in \mathcal{G}} \sum_{t \in \mathcal{T}} \left(K_g u_{gt} + S_g v_{gt} + \sum_{k \in \mathcal{K}} C_{gk} s_{gkt} \right) \quad (1a)$$

$$\text{s.t.} \quad \sum_{l \in \mathcal{L}_n^+} f_{lt} - \sum_{l \in \mathcal{L}_n^-} f_{lt} + \sum_{g \in \mathcal{G}_n} p_{gt} = D_{nt}, \quad n \in \mathcal{N}, t \in \mathcal{T}, \quad (1b)$$

$$f_{lt} = B_l (\theta_{nt} - \theta_{mt}), \quad l = (m, n) \in \mathcal{L}, t \in \mathcal{T}, \quad (1c)$$

$$p_{gt} = \sum_{k \in \mathcal{K}} s_{gkt}, \quad g \in \mathcal{G}, t \in \mathcal{T}, \quad (1d)$$

$$r_{gt}^- \leq p_{gt} \leq r_{gt}^+, \quad g \in \mathcal{G}, t \in \mathcal{T}, \quad (1e)$$

$$r_{gt}^+ \leq P_g^{max} u_{gt}, \quad g \in \mathcal{G}, t \in \mathcal{T}, \quad (1f)$$

$$r_{gt}^- \geq P_g^{min} u_{gt}, \quad g \in \mathcal{G}, t \in \mathcal{T}, \quad (1g)$$

$$\sum_{g \in \mathcal{G}} r_{gt}^+ \geq (1 + \gamma^+) \sum_{n \in \mathcal{N}} D_{nt}, \quad t \in \mathcal{T}, \quad (1h)$$

$$\sum_{g \in \mathcal{G}} r_{gt}^- \leq (1 - \gamma^-) \sum_{n \in \mathcal{N}} D_{nt}, \quad t \in \mathcal{T}, \quad (1i)$$

$$r_{gt}^+ - p_{g,t-1} \leq R_g^+ u_{g,t-1} + P_g^{max} v_{gt}, \quad g \in \mathcal{G}, t \geq 2, \quad (1j)$$

$$r_{gt}^- - p_{g,t-1} \geq -R_g^- u_{g,t-1} - P_g^{min} v_{gt}, \quad g \in \mathcal{G}, t \geq 2, \quad (1k)$$

$$\sum_{q=\max\{1, t-UT_g+1\}}^t v_{gq} \leq u_{gt}, \quad g \in \mathcal{G}, t \in \mathcal{T}, \quad (1l)$$

$$\sum_{q=\max\{1, t-DT_g+1\}}^t w_{gq} \leq 1 - u_{gt}, \quad g \in \mathcal{G}, t \in \mathcal{T}, \quad (1m)$$

$$v_{gt} - w_{gt} = u_{gt} - u_{g,t-1}, \quad g \in \mathcal{G}, t \geq 2, \quad (1n)$$

$$-F_l \leq f_{lt} \leq F_l, \quad l \in \mathcal{L}, t \in \mathcal{T}, \quad (1o)$$

$$\Theta_n^{min} \leq \theta_{nt} \leq \Theta_n^{max}, \quad n \in \mathcal{N}, t \in \mathcal{T}, \quad (1p)$$

$$u_{gt}, v_{gt}, w_{gt} \in \{0, 1\}, \quad g \in \mathcal{G}, t \in \mathcal{T}. \quad (1q)$$

The objective function (1a) of the problem is to minimize the sum of the commitment cost, the startup cost, and the generation cost. Constraint (1b) ensures the flow balance for each bus $n \in \mathcal{N}$ and time $t \in \mathcal{T}$. Constraint (1c) represents a linearized power flow equation based on Kirchhoff's law, modeling electricity transmission. Constraint (1d) splits power generation into price blocks $k \in \mathcal{K}$. Relations between reserve up/down and power generation are described by constraints (1e) – (1g); constraints (1f) and (1g) also represent on/off of each generator g at time t with specified generation capacities. Constraints (1h) and (1i) represent the spinning reserve requirements as a fraction of the total system load for each time period t . Constraints (1l) and (1m) ensure the minimum up- and downtime, respectively, for each generator. Equation (1n) describes the logic between commitment, startup, and shutdown decisions. Equations (1o) and (1p) are the bound constraints for transmission line capacity and phase angle,

respectively. Commitment, startup, and shutdown decision values are restricted to binaries by (1q). Note that more constraints can be added to the model (1), such as fuel and emission limits [7].

In practice, a PCM simulation oftentimes solves a set of UC models (1) on a rolling horizon basis with an overlapping period, e.g. solving the UC problem for two days, but keeping the solution for the first day only, and then move on to the next day. Constraints (1j) – (1n) couple multiple time periods. The results from the previous optimization problem determine the initial conditions (e.g., generator status, generation, and reserve amount) for the *coupling* constraints for the next planning period. In order to implement parallel PCM simulations, the rolling horizon approach can be replaced by solving many optimization problems for separate planning periods in parallel [5]. In this study, overlap periods ranging from 0 to 5 days at the beginning of the period were used to address the coupling constraints over time, resulting in individual optimization problems up to 168 hours. In particular, it was found that using a longer overlap period provide more accurate simulation solutions for PCM [5].

III. TEMPORAL DECOMPOSITION OF UC PROBLEM

While solving a longer-term UC problem (1) is important for accurate PCM simulation, solving a sequence of UC problems poses a significant computational challenge in PCM simulation. We present a decomposition approach that accelerates the UC solution time by decoupling problem (1) into a number of subproblems with smaller time horizons. The decomposition can be obtained by relaxing the coupling constraints (1j) – (1n). We also highlight that our decomposition approach is different from the time domain decomposition [5], which does not guarantee consistent solutions across subhorizons, whereas our approach guarantees an optimal solution for the long-term UC problem. We first define the set of subhorizon indices \mathcal{J} ,

- 1) $\mathcal{T}_j \subset \mathcal{T}$ for $j \in \mathcal{J}$,
- 2) $\cup_{j \in \mathcal{J}} \mathcal{T}_j = \mathcal{T}$, and
- 3) $\mathcal{T}_i \cap \mathcal{T}_j = \emptyset$ for $i \neq j \in \mathcal{J}$,

where \mathcal{T}_j is a subset of time horizon such that the indices for time periods are consecutive. Using the set \mathcal{J} , we rewrite the problem (1) to the following equivalent form with a set of coupling constraints and the others. We also define vectors $\mathbf{u}_j, \mathbf{v}_j, \mathbf{w}_j, \mathbf{p}_j, \mathbf{r}_j$, and \mathbf{s}_j , where the elements are respectively $u_{gt}, v_{gt}, w_{gt}, p_{gt}, r_{gt}$, and s_{gt} for $g \in \mathcal{G}, t \in \mathcal{T}_j$.

$$\min \sum_{j \in \mathcal{J}} \sum_{g \in \mathcal{G}} \sum_{t \in \mathcal{T}_j} \left(K_g u_{gt} + S_g v_{gt} + \sum_{k \in \mathcal{K}} C_{gk} s_{gkt} \right) \quad (2a)$$

$$\text{s.t.} \quad r_{gt}^+ - p_{g,t-1} \leq R_g^+ u_{g,t-1} + P_g^{max} v_{gt}, \quad g \in \mathcal{G}, t \in \mathcal{T}_j, t-1 \notin \mathcal{T}_j, j \in \mathcal{J}, \quad (2b)$$

$$r_{gt}^- - p_{g,t-1} \geq -R_g^- u_{g,t-1} - P_g^{min} v_{gt}, \quad g \in \mathcal{G}, t \in \mathcal{T}_j, t-1 \notin \mathcal{T}_j, j \in \mathcal{J}, \quad (2c)$$

$$\sum_{q=\max\{1, t-UT_g+1\}}^t v_{gq} \leq u_{gt}, \quad g \in \mathcal{G}, t \in \mathcal{T}_j, t-UT_g+1 \notin \mathcal{T}_j, j \in \mathcal{J}, \quad (2d)$$

$$\begin{aligned}
 \sum_{q=\max\{1,t-DT_g+1\}}^t w_{gq} &\leq 1 - u_{gt}, \\
 g \in \mathcal{G}, t \in \mathcal{T}_j, t - DT_g + 1 \notin \mathcal{T}_j, j \in \mathcal{J}, \quad (2e) \\
 v_{gt} - w_{gt} &= u_{gt} - u_{g,t-1}, \\
 g \in \mathcal{G}, t \in \mathcal{T}_j, t - 1 \notin \mathcal{T}_j, j \in \mathcal{J}, \quad (2f) \\
 (\mathbf{u}_j, \mathbf{v}_j, \mathbf{w}_j, \mathbf{p}_j, \mathbf{r}_j, \mathbf{s}_j) &\in \mathcal{X}_j, j \in \mathcal{J}. \quad (2g)
 \end{aligned}$$

Here constraints (2b)–(2f) couple two consecutive subhorizons, and \mathcal{X}_j is the set of feasible solutions defined by all the noncoupling constraints for subhorizon j ; that is,

$$\begin{aligned}
 \sum_{l \in \mathcal{L}_n^+} f_{lt} - \sum_{l \in \mathcal{L}_n^-} f_{lt} + \sum_{g \in \mathcal{G}_n} p_{gt} &= D_{nt}, n \in \mathcal{N}, t \in \mathcal{T}_j, \\
 f_{lt} &= B_l(\theta_{nt} - \theta_{mt}), l = (m, n) \in \mathcal{L}, t \in \mathcal{T}_j, \\
 p_{gt} &= \sum_{k \in \mathcal{K}} s_{gkt}, g \in \mathcal{G}, t \in \mathcal{T}_j, \\
 r_{gt}^- &\leq p_{gt} \leq r_{gt}^+, g \in \mathcal{G}, t \in \mathcal{T}_j, \\
 r_{gt}^+ &\leq P_g^{max} u_{gt}, g \in \mathcal{G}, t \in \mathcal{T}_j, \\
 r_{gt}^- &\geq P_g^{min} u_{gt}, g \in \mathcal{G}, t \in \mathcal{T}_j, \\
 \sum_{g \in \mathcal{G}} r_{gt}^+ &\geq (1 + \gamma^+) \sum_{n \in \mathcal{N}} D_{nt}, t \in \mathcal{T}_j, \\
 \sum_{g \in \mathcal{G}} r_{gt}^- &\leq (1 - \gamma^-) \sum_{n \in \mathcal{N}} D_{nt}, t \in \mathcal{T}_j, \\
 r_{gt}^+ - p_{g,t-1} &\leq R_g^+ u_{g,t-1} + P_g^{max} v_{gt}, g \in \mathcal{G}, (t-1), t \in \mathcal{T}_j, \\
 r_{gt}^- - p_{g,t-1} &\geq -R_g^- u_{g,t-1} - P_g^{min} v_{gt}, g \in \mathcal{G}, (t-1), t \in \mathcal{T}_j, \\
 \sum_{q=\max\{\min\{\mathcal{T}_j\}, t-UT_g+1\}}^t v_{gq} &\leq u_{gt}, g \in \mathcal{G}, t \in \mathcal{T}_j, \\
 \sum_{q=\max\{\min\{\mathcal{T}_j\}, t-DT_g+1\}}^t w_{gq} &\leq 1 - u_{gt}, g \in \mathcal{G}, t \in \mathcal{T}_j, \\
 v_{gt} - w_{gt} &= u_{gt} - u_{g,t-1}, g \in \mathcal{G}, (t-1), t \in \mathcal{T}_j, \\
 -F_l &\leq f_{lt} \leq F_l, l \in \mathcal{L}, t \in \mathcal{T}_j, \\
 \Theta_n^{min} &\leq \theta_{nt} \leq \Theta_n^{max}, n \in \mathcal{N}, t \in \mathcal{T}_j, \\
 u_{gt}, v_{gt}, w_{gt} &\in \{0, 1\}, g \in \mathcal{G}, t \in \mathcal{T}_j.
 \end{aligned}$$

Before deriving the decomposition framework, we further simplify the formulation of problem (2). We define the decision variable vectors \mathbf{x}_j such that \mathbf{x}_j concatenate $(u_t, v_t, w_t, p_t, r_t, s_t)$ for $t \in \mathcal{T}_j$. In particular, \mathbf{x}_j represents the decision variables for subhorizon j . Problem (2) can be written as

$$z := \min \sum_{j \in \mathcal{J}} \mathbf{c}_j \mathbf{x}_j \quad (3a)$$

$$\text{s.t. } \sum_{j \in \mathcal{J}} \mathbf{A}_j \mathbf{x}_j \geq \mathbf{b}, \quad (3b)$$

$$\mathbf{x}_j \in \mathcal{X}_j, j \in \mathcal{J}, \quad (3c)$$

where the objective coefficient vectors \mathbf{c}_j are defined to represent (2a), and constraint (3b) represents constraints (2b)–(2f) that couple the subhorizons.

We present the flowchart of the temporal decomposition method in Figure 1, where each of the main elements is described in the following sections. The temporal decomposition

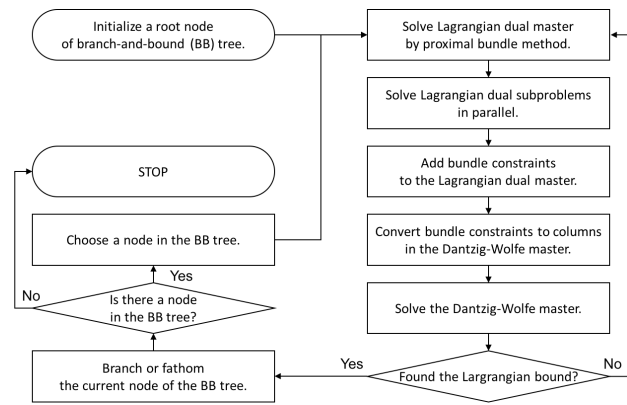


Fig. 1. Flowchart of the Temporal Decomposition Method.

is based on dual decomposition (DD) III-A and Dantzig-Wolfe decomposition (DWD) III-B for finding lower bounds, whereas primal solutions are found using a branch-and-bound (BB) method III-C. The flowchart starts by initializing a root node of the BB tree. The right-hand side of the chart represents the lower bounding procedure by the DD and DWD. The lower left part represents the BB procedure.

A. Lower Bounding from Dual Decomposition

We present the Lagrangian dual of problem (3) resulting from the Lagrangian relaxation of constraint (3b). We define the Lagrangian dual function as

$$\mathcal{L}(\lambda) := \mathbf{b}\lambda + \sum_{j \in \mathcal{J}} D_j(\lambda), \quad (4)$$

where λ is the dual variable corresponding to constraint (3b) and $D_j(\lambda)$ is defined as

$$D_j(\lambda) := \min_{\mathbf{x}_j \in \text{conv}(\mathcal{X}_j)} (\mathbf{c}_j - \lambda^T \mathbf{A}_j) \mathbf{x}_j. \quad (5)$$

The Lagrangian dual bound is obtained by solving

$$z_{LD} := \max_{\lambda \geq 0} \mathcal{L}(\lambda). \quad (6)$$

Note that $z \geq z_{LD} \geq z_{LP}$, where z_{LP} is the optimal objective value of the linear relaxation of problem (3). Problem (6) can be solved by a number of algorithms, such as the subgradient method and bundle method (see [10] and references therein).

We use a proximal bundle method (e.g., [20]) that outer-approximates the Lagrangian dual function $\mathcal{L}(\lambda)$ by adding linear inequalities with a regularization term of ℓ_2 -norm in the objective function. A set of linear inequalities is added at each iteration k . Let κ be the index for current iteration. After adding κ sets of linear inequalities, the dual master problem (DMP) of the proximal bundle method is given by

$$\max \sum_{j \in \mathcal{J}} \mu_j + \mathbf{b}\lambda + \frac{1}{2\tau} \|\lambda - \hat{\lambda}\|_2^2 \quad (7a)$$

$$\text{s.t. } \mu_j \leq D_j(\lambda^k) + (\mathbf{A}_j \mathbf{x}_j^k)^T (\lambda - \lambda^k), \quad (7b)$$

$$j \in \mathcal{J}, k = 1, \dots, \kappa, \quad (7b)$$

$$\lambda \geq 0, \quad (7c)$$

where τ is a positive constant and $\hat{\lambda}$ is the proximal center. Constraints (7b) are the linear inequalities that construct the outer-approximation of $\mathcal{L}(\lambda)$.

Algorithm 1 Dual Decomposition

Require: Initialize $\mathbf{c}_j, \mathbf{A}_j, \mathcal{X}_j, \mathbf{b}, \tau > 0, \hat{\lambda} \geq 0$, and $\epsilon \geq 0$.
 Set $\lambda^1 \leftarrow \hat{\lambda}, \kappa \leftarrow 1$, and $z_{LB} \leftarrow -\infty$.

- 1: **loop**
- 2: Solve (5) for given λ^κ and for each $j \in \mathcal{J}$.
- 3: Stop if $\mathcal{L}(\lambda^\kappa) - z_{LB} < \epsilon$
- 4: Update the best bound z_{LB} , the proximal center $\hat{\lambda}$, and weight τ .
- 5: Find an optimal solution $(\lambda^{\kappa+1}, \mu_j^{\kappa+1})$ of (7).
- 6: Set $\kappa \leftarrow \kappa + 1$.
- 7: **end loop**
- 8: **return** z_{LB} and \mathbf{x}_j^k for $j \in \mathcal{J}$ and $k = 1, \dots, \kappa$.

We summarize the algorithmic steps of the proximal bundle method in Algorithm 1. The algorithm is initialized with problem data and parameters. Solving subproblems (5) at line 2 finds a new dual bound and generates linear inequalities (7b) for given λ^κ . To update $z_{LB}, \hat{\lambda}$, and τ at line 4, we follow Algorithm 2.1 and Procedure 2.2 in [20]. We solve the DMP (7) by adding the linear inequalities with the proximal parameters $\hat{\lambda}$ and τ . We repeat the steps 2 – 6 until the stopping criterion in line 3 is satisfied. Note that $z_{LD} \geq \mathcal{L}(\lambda^k) \geq \mathcal{L}(\lambda^{k-1})$ for $k = 2, \dots, \kappa$. The convergence of the algorithm depends on step 4 and is proved in [20].

B. Dantzig-Wolfe Decomposition

While effectively finding a tight dual bound z_{LD} of z , the DD does not find a primal bound of the problem (i.e., a primal feasible solution). In production cost modeling, finding a primal optimal solution is necessary for analyzing the electric grid system. DWD is a primal-dual pair of the DD, which constructs an inner-estimate of the convex hull of \mathcal{X}_j (denoted by $\text{conv}(\mathcal{X}_j)$) for $j \in \mathcal{J}$. We apply the decomposition to problem (3) by considering constraint (3b) only and estimating (3c). In particular, we define the restricted master problem (RMP) that considers constraint (3b) only for a limited number of solutions $\mathbf{x}_j \in \text{conv}(\mathcal{X}_j)$ for each $j \in \mathcal{J}$. Then, we use \mathbf{x}_j^k from the pricing problem of the DD. Therefore, for given $\mathbf{x}_j^k, j \in \mathcal{J}, k = 1, \dots, \kappa$, the RMP is given by

$$z_{DW} := \min \sum_{j \in \mathcal{J}} \sum_{k=1}^{\kappa} \mathbf{c}_j \mathbf{x}_j^k \alpha_j^k \quad (8a)$$

$$\text{s.t.} \sum_{j \in \mathcal{J}} \sum_{k=1}^{\kappa} \mathbf{A}_j \mathbf{x}_j^k \alpha_j^k \geq \mathbf{b}, \quad (8b)$$

$$\sum_{k=1}^{\kappa} \alpha_j^k = 1, j \in \mathcal{J}, \quad (8c)$$

$$\alpha_j^k \geq 0, j \in \mathcal{J}, k = 1, \dots, \kappa. \quad (8d)$$

Note that the feasible solutions to problem (3) are approximated by the convex combination of $\mathbf{x}_j^k \in \text{conv}(\mathcal{X}_j)$. The original variable solution is obtained by $\mathbf{x}_j = \sum_{k=1}^{\kappa} \mathbf{x}_j^k \alpha_j^k$

for $j \in \mathcal{J}$. In addition, the RMP is a linear programming problem. Let λ and μ_j be the dual variables corresponding to constraints (8b) and (8c), respectively.

C. Branch-and-Bound Method

Recall that some of the elements in the original variable vector $\mathbf{x}_j = \sum_{k=1}^{\kappa} \mathbf{x}_j^k \alpha_j^k$ are restricted to being binaries. However, RMP does not necessarily find a binary feasible solution of the original problem (3). We apply the BB method for ensuring a binary feasible solution by the branching procedure. Let $\hat{\alpha}_j^k$ be an optimal solution of RMP. For given fractional value of $\sum_{k=1}^{\kappa} \mathbf{x}_j^k \hat{\alpha}_j^k$ at a node of the BB tree, the branching procedure creates two child nodes by adding the branching hyperplanes

$$\sum_{k=1}^{\kappa} \mathbf{x}_j^k \alpha_j^k \leq \lfloor \sum_{k=1}^{\kappa} \mathbf{x}_j^k \hat{\alpha}_j^k \rfloor \text{ and } \sum_{k=1}^{\kappa} \mathbf{x}_j^k \alpha_j^k \geq \lceil \sum_{k=1}^{\kappa} \mathbf{x}_j^k \hat{\alpha}_j^k \rceil \quad (9)$$

to each of the child nodes, respectively. Note that adding a branching hyperplane is equivalent to branching on a fractional variable \mathbf{x}_j of the original problem (3). Then, the BNP method chooses a new node from the BNP tree and solves the node problem by using Algorithm 1.

Algorithm 2 Branch-and-Bound Method

Require: Initialize the problem data $\mathbf{c}_j, \mathbf{A}_j, \mathcal{X}_j, \mathbf{b}$, upper bound $z_{UB} \leftarrow \infty$, and $\text{TREE} \leftarrow \emptyset$.

- 1: Create a root node (Node⁰) for given $\mathbf{c}_j, \mathbf{A}_j, \mathcal{X}_j, \mathbf{b}$, and $\text{TREE} \leftarrow \text{TREE} \cup \{\text{Node}^0\}$.
- 2: **repeat**
- 3: Choose a node Node $\in \text{TREE}$.
- 4: Update $\text{TREE} \leftarrow \text{TREE} \setminus \{\text{Node}\}$
- 5: Call Algorithm 1 for solving the DMP of Node, which returns z_{LB} and \mathbf{x}_j^k .
- 6: Solve the RMP of Node that finds $\hat{\alpha}_j^k$ for given \mathbf{x}_j^k .
- 7: **if** $\sum_{k=1}^{\kappa} \mathbf{x}_j^k \hat{\alpha}_j^k$ is fractional **then**
- 8: Choose an original variable to branch.
- 9: Create two nodes (Node^L and Node^R) by adding each of (9) corresponding to the branching variable.
- 10: Update $\text{TREE} \leftarrow \text{TREE} \cup \{\text{Node}^L, \text{Node}^R\}$.
- 11: **else**
- 12: Update $z_{UB} \leftarrow \min\{z_{UB}, z_{LB}\}$.
- 13: **end if**
- 14: **until** $\text{TREE} = \emptyset$

We also summarize the algorithmic steps of the BB method in Algorithm 2. In the initialization step of the algorithm, the BNP tree is initialized as an empty set TREE of nodes (line 1). Any Node $\in \text{TREE}$ represents the problem data for the nodes that are not solved in the algorithm. The root node that represents the initial problem of the algorithm is created in line 2. The algorithm repeats lines 3 – 13 until no node exists in TREE. A node is chosen and removed from TREE in lines 3 and 4, respectively. For any node chosen in line 3, Algorithm 2 solves the DMP and RMP of the node in lines 5 and 6. In line 9, adding the branching hyperplanes (9) to each of the nodes is equivalent to updating the problem data \mathbf{A}_j and \mathbf{b} . The BNP algorithm terminates with $z = z_{UB}$ and returns the corresponding primal solution $\mathbf{x}_j = \sum_{k=1}^{\kappa} \mathbf{x}_j^k \hat{\alpha}_j^k$ for $j \in \mathcal{J}$.

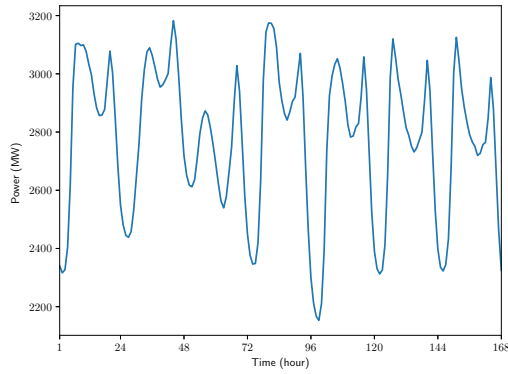


Fig. 2. Load profile used for the IEEE 118-bus system.

IV. COMPUTATIONAL RESULTS

We present computational results for using the temporal decomposition method on test problems. We have implemented the temporal decomposition method in an open-source decomposition solver DSP [10], which can run on high-performance computing clusters in parallel via the MPI library. In addition, we have integrated a branch-and-bound (BB) method on top of the temporal decomposition method, which allows us to find an optimal solution to the original problem (1), as compared with finding lower bounds only. For the BB method (Algorithm 2), we have utilized an open-source software package Coin-ALPS [21] that implements a generic tree search framework. DSP uses a commercial optimization solver CPLEX (version 12.7) for solving the mixed-integer programming subproblems (5) of the temporal decomposition. We have modeled the problem (1) and its decomposition in the Julia script language, which can be read by DSP. All the computations were run on *Blues*, a 630-node computing cluster at Argonne National Laboratory. The *Blues* cluster has a QLogic QDR InfiniBand network, and each node has two octo-core 2.6 GHz Xeon processors and 64 GB of RAM. Note, however, that our implementation can also run on a laptop or workstation.

A. IEEE 118-Bus System

We use the IEEE 118-bus system with 118 buses, 54 generators, and 186 transmission lines. The system has a total generation capacity of 5,450 MW. The system is required to reserve 10% and 5% of the system load as spinning up/down reserves for the ability to increase and decrease the generation, respectively (i.e., $\gamma^+ = 0.1$ and $\gamma^- = 0.05$). We also consider three blocks of generation cost (i.e., $|\mathcal{K}| = 3$). Figure 2 shows the fluctuation of the system load profile used in our study. We use seven days of the load profile with 1-hour intervals. In particular, we use the estimated hourly load of the PJM system [22] for the dates from April 8 to April 14, 2016, which is scaled down to 10% to obtain the load profile used in our computational study. The load is 2,775 MW on average, with a peak of 3,182 MW.

1) *Extensive Form Solutions*: Table I presents the size of the problem instances for 24-, 48-, 72-, 96-, 120-, 144-, and

TABLE I
SIZES OF IEEE 118-BUS SYSTEM PROBLEM INSTANCES

T	# Constraints	# Variables	# Binary
24	19765	18960	1296
48	40070	37920	2592
72	60398	56880	3888
96	80726	75840	5184
120	101054	94800	6480
144	121382	113760	7776
168	141710	132720	9072

TABLE II
NUMERICAL RESULTS FOR PROBLEM INSTANCES USING CPLEX-12.7 IN PARALLEL WITH 16 COMPUTING CORES

T	Best Objective	Gap (%)	Time (sec.)
24	1077030.3	0	6
48	2171642.3	0	68
72	3122813.6	0	1351
96	4174770.7	< 0.01	14400
120	5158594.4	< 0.01	14400
144	6152020.7	0.01	14400
168	7122822.5	0.02	14400

168-hour horizons. Recall that the 168-horizon UC problem represents the 24-hour operation horizon with 6 days of overlap (lookahead) for the PCM simulation. The UC problem is solved up to a week ahead in their operational decision processes to account for generating units with very long startup times [23]. Table II summarizes the numerical results for each problem instance solved by CPLEX in parallel on a 16-core single node of the *Blues* cluster. We set a zero optimality gap tolerance and a 4-hour wall clock time limit. The smallest objective function values of all feasible solutions found are reported in “Best Objective” with the relative gap (“Gap”) between the best objective value and the best lower bound. Within the time limit, optimal objective values were found for 24-, 48-, and 72-hour problem instances. For the other problem instances, CPLEX found solutions with gaps. In particular, the optimality gap increases as the problem size increases, as shown in Table II.

2) *Temporal Decomposition Solutions*: We now present the numerical results from the temporal decomposition. We tested the decomposition method with different numbers of subhorizons (i.e., $|\mathcal{J}| = 2, 4, 8, 12, 24$). We used the weight parameter $\tau = 1000$, the initial dual variable values of zero for λ , and the stopping tolerance $\epsilon = 10^{-6}$ in Algorithm 1. Table III provides insights into the inner working of the decomposition algorithm by showing the size of the coupling problem (2) that results for different optimization periods and subhorizons. The percentages of the coupling constraints and variables to the total numbers are also reported in the table. The number of constraints, all variables, and binary variables increases with the number of decompositions. However, we highlight that the temporal decomposition generates columns iteratively up to the number of coupling variables reported in Table III. Therefore, the size of the master problem is far smaller than the size of the coupling problem.

In Figure 3 and Table IV, we report numerical results from the temporal decomposition method with different numbers of subintervals for 24-, 48-, 72-, 96-, 120-, 144-, and 168-horizon

TABLE III

NUMBER OF COUPLING CONSTRAINTS, ALL VARIABLES, AND BINARY VARIABLES. PERCENTAGES OF THE TOTAL NUMBERS OF ORIGINAL CONSTRAINTS, VARIABLES, AND BINARY VARIABLES (REPORTED IN PARENTHESES).

T	$ \mathcal{J} $	Constraints	All variables	Binary variables
24	2	594 (3%)	3456 (18%)	702 (54%)
	4	1506	4104	1026
	8	2548	4914	1188
	12	3300	5616	1242
	24	5428 (27%)	7614 (40%)	1296 (100%)
48	2	617 (1%)	6588 (17%)	1350 (52%)
	4	1782	7668	1998
	8	3514	8640	2322
	12	4510	9396	2430
	24	6900 (17%)	11448 (30%)	2538 (97%)
72	2	629 (1%)	8532 (15%)	1998 (51%)
	4	1818	11232	2970
	8	4032	12366	3456
	12	5522	13176	3618
	24	8372 (13%)	15282 (26%)	3780 (97%)
96	2	640 (0.7%)	10314 (13%)	2592 (50%)
	4	1851	14688	3942
	8	4158	16092	4590
	12	6182	16956	4806
	24	9430 (11%)	19116 (25%)	5022 (96%)
120	2	640 (0.6%)	10314 (10%)	2592 (40%)
	4	1869	17604	4914
	8	4200	19818	5724
	12	6424	20736	5994
	24	10488 (10%)	22950 (24%)	6264 (96%)
144	2	640 (0.5%)	10314 (9%)	2592 (33%)
	4	1887	20520	5886
	8	4242	23544	6858
	12	6534	24516	7182
	24	11546 (9%)	26784 (20%)	7506 (96%)
168	2	640 (0.4%)	10314 (7%)	2592 (28%)
	4	1905	23436	6858
	8	4284	27270	7992
	12	6578	28296	8370
	24	12604 (8%)	30618 (23%)	8748 (96%)

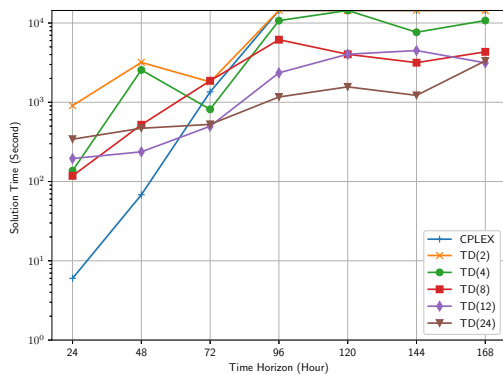


Fig. 3. Solution times resulting from the temporal decompositions for different numbers of time periods.

UC problems. The temporal decomposition (Algorithm 2) solves the MIP pricing subproblem (5) for each $j \in \mathcal{J}$ in parallel. Each subproblem is solved on a single node with 16 cores. For example, the problem of $|\mathcal{J}| = 24$ solves 24 subproblems on 24 computing nodes with 384 ($=24 \cdot 16$) cores. The quadratic programming master problem is also solved in parallel by CPLEX on a single node with 16 cores. We also set 4-hour total time limit for these runs.

Figure 3 plots the solution times resulting from CPLEX

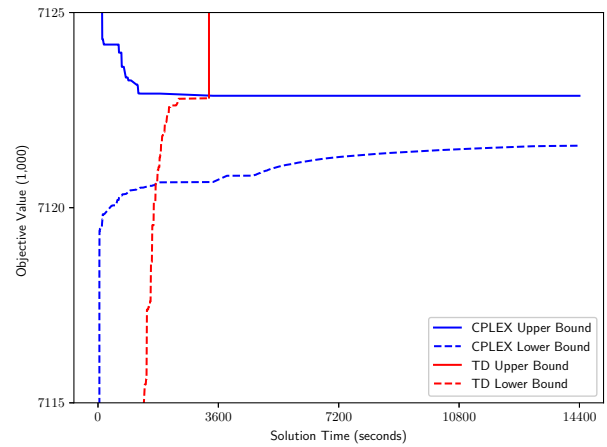


Fig. 4. Progress on the lower and upper bounds for solving the 168-hour unit commitment problem of the IEEE 118-bus system by CPLEX and the temporal decomposition TD(24).

and the temporal decomposition method with different numbers of subintervals. The x-axis presents the time horizon of the UC problem. “TD(n)” plots the solution time from the temporal decomposition of n subintervals for $n = 2, 4, 8, 12, 24$. The temporal decomposition method found optimal solutions for all the problem instances (i.e., $T = 24, 48, 72, 96, 120, 144, 168$) within the time limit, except for the case where $n = 2$, which did not solve to optimality for time horizons longer than 72 hours, and for $n = 4$, which did not solve to optimality for time horizon of 120 hours. In particular, the 96-hour horizon problem was solved to optimality after 1166 seconds when decomposed into 24 subhorizons. Therefore, for this problem instance, since CPLEX could not find an optimal solution in 4 hours (14400sec), the solution time was reduced by at least a factor of 12 by using temporal decomposition.

In Figure 4, we present how the lower and upper bounds progress in CPLEX and the temporal decomposition method. CPLEX found lower and upper bound early in the solution progress. In particular, CPLEX is able to find a good upper bound (i.e., a primal feasible solution) by running a number of heuristic algorithms, whereas steadily improving the lower bounds by the BB method. In contrast, the temporal decomposition found a good lower bound by the DD and primal feasible solutions later than the BB method, but it closes the gap and finds the optimal solution much faster.

Detailed numerical results are reported in Table IV. The columns for “Root Node” present the results observed at the root node before starting the BB method. The column “Iterations” reports the number of iterations taken in Algorithm 1. The best lower bound of z are reported in the column “Best Bound” with the relative gap as the relative difference between the best bound and the best objective found by CPLEX as reported in Table II. For the BB results in Table IV, “Nodes” reports the number of BB nodes solved. “Best Objective” reports the objective value of the primal solution. Note that the temporal decomposition found the optimal solutions and the best objective values for all the problem instances, as opposed to CPLEX which could not solve to full optimality

TABLE IV
NUMERICAL RESULTS FROM TEMPORAL DECOMPOSITION WITH DIFFERENT NUMBER OF SUB-HORIZONS.

T	$ \mathcal{J} $	Root Node				Branch-and-Bound				
		Iterations	Best Bound	Gap (%)	Time (sec.)	Nodes	Best Bound	Best Objective	Gap (%)	Time (sec.)
24	2	17	1077030.3	0	908	1	1077030.3	1077030.3	0	908
	4	54	1077030.3	0	137	1	1077030.3	1077030.3	0	137
	8	92	1077023.6	< 0.01	103	5	1077030.3	1077030.3	0	118
	12	120	1077030.3	0	148	13	1077030.3	1077030.3	0	195
	24	140	1077023.0	< 0.01	237	13	1077030.3	1077030.3	0	342
48	2	49	2171629.6	< 0.01	2092	11	2171642.3	2171642.3	0	3187
	4	71	2171623.1	< 0.01	2526	3	2171642.3	2171642.3	0	2559
	8	90	2171620.9	< 0.01	435	5	2171642.3	2171642.3	0	520
	12	105	2171622.2	< 0.01	176	13	2171642.3	2171642.3	0	237
	24	129	2171635.1	< 0.01	237	35	2171642.3	2171642.3	0	470
72	2	32	3122813.6	0	1941	1	3122813.6	3122813.6	0	1807
	4	37	3122800.0	< 0.01	858	11	3122813.6	3122813.6	0	815
	8	65	3122792.5	< 0.01	1289	11	3122813.6	3122813.6	0	1868
	12	87	3122810.3	< 0.01	436	19	3122813.6	3122813.6	0	498
	24	129	3122806.5	< 0.01	299	15	3122813.6	3122813.6	0	526
96	2	48	4174726.5	< 0.01	14400	0	4174726.5	NA	< 0.01	14400
	4	47	4174746.5	< 0.01	3803	19	4174770.7	4174770.7	0	10730
	8	84	4174763.3	< 0.01	4247	35	4174770.7	4174770.7	0	6160
	12	112	4174747.4	< 0.01	1473	33	4174770.7	4174770.7	0	2352
	24	141	4174769.4	< 0.01	735	29	4174770.7	4174770.7	0	1166
120	2	48	5158553.5	< 0.01	14400	0	5158553.5	NA	< 0.01	14400
	4	55	5144130.4	0.28	14400	0	5144130.4	NA	0.28	14400
	8	99	5158562.0	< 0.01	3148	5	5158594.4	5158594.4	0	4033
	12	116	5158568.2	< 0.01	3355	15	5158594.4	5158594.4	0	4039
	24	129	5158570.9	< 0.01	829	35	5158594.4	5158594.4	0	1565
144	2	47	6150192.3	0.03	14400	0	6150192.3	NA	0.03	14400
	4	65	6151935.2	< 0.01	7108	3	6151974.0	6151974.0	0	7646
	8	77	6151928.5	< 0.01	1967	15	6151974.0	6151974.0	0	3161
	12	96	6151934.4	< 0.01	3560	19	6151974.0	6151974.0	0	4494
	24	139	6151933.5	< 0.01	1057	7	6151974.0	6151974.0	0	1222
168	2	47	7119965.0	0.04	14400	0	7119965.0	NA	0.04	14400
	4	57	7122821.1	< 0.01	10573	1	7122821.1	7122821.1	0	10753
	8	98	7122771.9	< 0.01	3600	0	7122821.1	7122821.1	0	4329
	12	108	7122773.7	< 0.01	2893	5	7122821.1	7122821.1	0	3145
	24	151	7122793.8	< 0.01	2396	15	7122821.1	7122821.1	0	3327

for time horizons beyond 72 hours. We highlight that the best bound found at the root node is very tight, with the gap less than 0.01% for most problem instances, including zero gaps for four of the instances. As a result, only a few of the BB nodes were solved to find a primal solution and prove optimality, as shown in the "Nodes" column. Note, however, that the computational performance depends on the choice of the number of subhorizons and that the best objective values were not found within the time limit (denoted by "NA") when the subproblems were large (e.g., the 96-horizon instance with $|\mathcal{J}| = 2$).

3) *Differences in Unit Commitment Solutions:* We highlight that unit commitment decisions are considerably different, when closing the 0.02% optimality gap for the 168-hour planning instance. Figure 5 plots the commitment schedules obtained by CPLEX and our temporal decomposition for the 168-hour time horizon instance. Specifically, the commitment schedules are different in 9 of the 54 generating units (17%) for 372 hours. Similar to Figure 5, we plot the absolute difference in power generation for each generating unit over the 168-hour horizon in Figure 6. The power generations are different in 26 of the 54 generating units (48%) with the maximum difference of 128.05 MWh and the total difference of 12,721 MW for the 168-hour horizon of all units. These results suggest that suboptimal schedules (even with small optimality gap) can deviate significantly from an optimal

TABLE V
COMPUTATIONAL PERFORMANCE FROM A ROLLING HORIZON SIMULATION FOR THE 168-HOUR UNIT COMMITMENT PROBLEM INSTANCE

T	Objective	Error (%)	Time (sec.)
24	7632690.3	6.68	25
48	7433805.6	4.18	264
72	7260291.1	1.89	3587

schedule and generation profile, thus hindering high-fidelity PCM simulations.

4) *Rolling Horizon Solutions and Errors:* A common approach in PCM is to use a rolling horizon to simulate the operation of the power system over multiple days. We conclude this section by showing that a rolling horizon approach produces substantial scheduling errors by implementing sub-optimal solutions to the original planning horizon. Table V reports the numerical results from using a rolling horizon approach that simulates the 168-hour unit commitment model with 24-, 48-, and 72-hour time windows. For example with the 24-hour time window, we solve the first 24 hours of the 168-hour horizon and fix the optimal solution for the first 24-hour time window. The optimal solution is used as the initial condition (e.g., number of hours generators are on/off, generation dispatch schedules) for the next 24-hour time window. Likewise, with the 48-hour window the model is also solved daily, only considering the results from the first

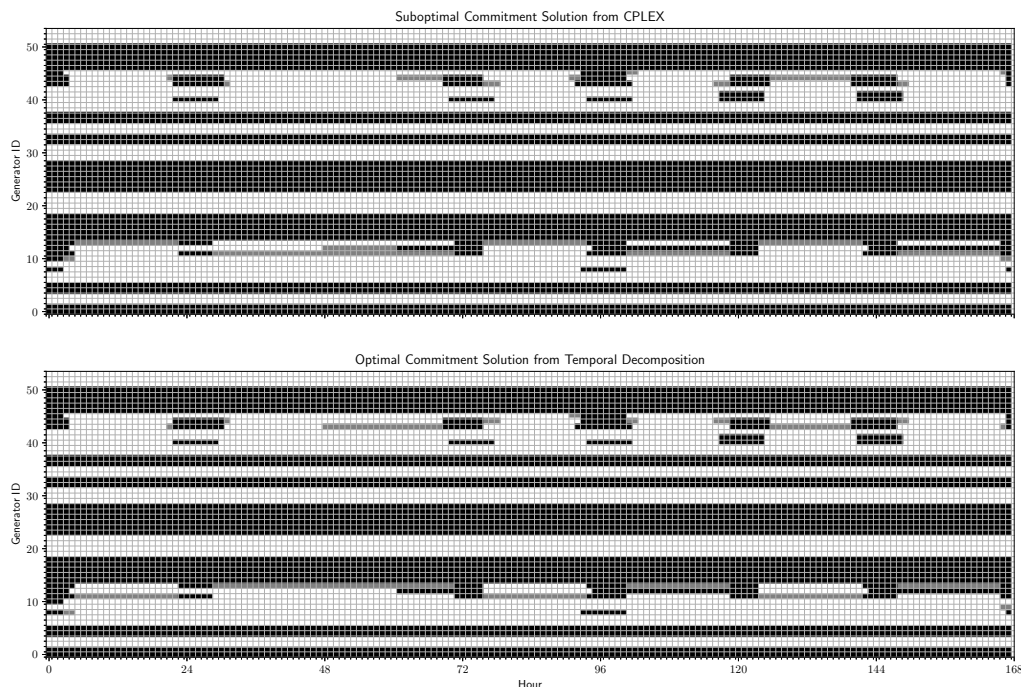


Fig. 5. Unit commitment solutions found for the 168-hour unit commitment problem instance by CPLEX and the temporal decomposition TD(24). The generators are scheduled online for the black-colored time periods with the gray highlights of differences.

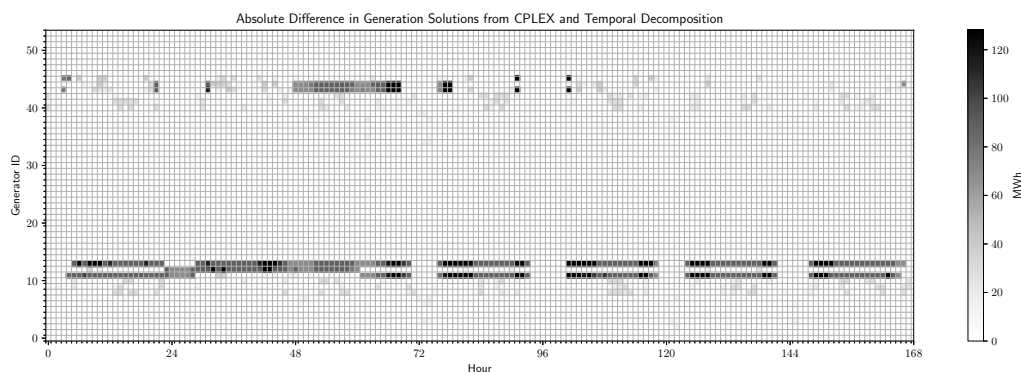


Fig. 6. Absolute difference in power generation found for the 168-hour unit commitment problem instance by CPLEX and the temporal decomposition TD(24). Darker plot is used for larger differences in MWh.

24 hours in each of the 7 days. In Table V, “Objective” is the sum of the optimal objective values for the time windows with the rolling horizon approach. “Error” calculates the difference between the “Objective” value and the optimal objective value of the 168-hour horizon UC problem as found by the temporal decomposition method (i.e., 7122821.1). Table V shows that a smaller time window produces a larger gap, which emphasizes the importance of using the optimal solution for a longer-term horizon. In particular, the 72-hour time window solution with the rolling horizon approaches produces an error that is nearly 2% and is even slower than the temporal decomposition solution for the full 168 hour period.

B. PEGASE 1354-Bus System

We consider a larger system from the Pan European Grid Advanced Simulation and State Estimation (PEGASE) project, with 1,354 buses, 260 generators of 128,738 MW total capacity, and 1,991 transmission lines [24]. The load is 7,548 MW

on average, with a peak of 9,450 MW. As in the IEEE 118-bus system case, we use 10% and 5% of the system load as spinning up/down reserves, respectively and consider three blocks of generation cost for each unit. Table VI presents the number of constraints, variables, and binary variables for each time horizon T . We highlight that the problem instances for the PEGASE 1354-bus system are seven times larger than those for the IEEE 118-bus system (in Table I).

Table VII shows the numerical results from CPLEX-12.7 solving the PEGASE 1354-bus problem instances with 24-, 48-, 72, 96-, 120-, 144-, and 168-hour horizons. The 24-, 48-, 72-, and 96-hour problem instances were solved to optimum within the 4-hour time limit. The other larger instances found “Best Objective” (i.e., upper bounds) with gaps.

We present the computational performance of the temporal decomposition solving the problem instances in parallel. The original time horizon was decomposed to 24 subhorizons for each problem instance. The problem instances reported lower

TABLE VI
SIZES OF PEGASE 1354-BUS SYSTEM PROBLEM INSTANCES

T	# Constraints	# Variables	# Binary
24	142232	136440	6240
48	284984	272880	12480
72	427736	409320	18720
96	570488	545760	24960
120	713240	682200	31200
144	855992	818640	37440
168	998744	955080	43680

TABLE VII
NUMERICAL RESULTS FOR THE PEGASE 1354-BUS INSTANCES USING CPLEX-12.7 IN PARALLEL WITH 16 COMPUTING CORES

T	Best Objective	Gap (%)	Time (sec.)
24	746057.9	0	196
48	1715371.6	0	2049
72	2561916.1	0	5581
96	3470853.9	0	10968
120	4217676.0	0.08	14400
144	5169400.5	0.12	14400
168	6122984.8	0.18	14400

TABLE VIII
COMPUTATIONAL PERFORMANCE FOR SOLVING THE PEGASE 1354-BUS INSTANCES USING THE TEMPORAL DECOMPOSITION TD(24)

T	Iterations	Best Bound	Gap (%)	Time (sec.)	
				Master	Total
24	249	744651.4	0.18	14165	14400
48	160	1710995.5	0.25	14184	14400
72	240	2558455.4	0.13	12855	14400
96	127	3460915.7	0.28	13184	14400
120	243	4214335.0	0.07	10746	14400
144	215	5163879.0	0.10	9893	14400
168	211	6115157.5	0.12	8218	14400

bounds in “Best Bound” with gaps that calculate the relative difference between the lower bounds and “Best Objective” in Table VII. However, for all the problem instances, the temporal decomposition terminated at root node solutions without any branching step due to the time limit. More importantly, we found that the master problem solutions become a significant bottleneck of the temporal decomposition when solving a very large-scale system with a larger number of coupling constraints (e.g., 60,606 coupling constraints for the 168-hour problem instance). For instance, for the 24-hour problem instance, 98% of the solution time was spent on solving the master problem. Note that this challenge has already been identified in the optimization community and addressed by developing a parallelization of the master solution [25], [26], reporting promising scalability results (e.g., 16 times speedup with 32 cores, as reported in [26]).

The temporal decomposition still provided substantially better lower bounds than did CPLEX for the 120-, 144-, and 168-hour problem instances (e.g., 0.12% vs. 0.18% for the 168-hour instance in Table VII). Figure 7 shows the progress on lower and upper bounds when solving the 168-hour problem instance by CPLEX and the temporal decomposition. The temporal decomposition found a good initial lower bound and improved it over time. In particular, the lower bounds from the temporal decomposition were always better than those from CPLEX. However, no upper bound was found because

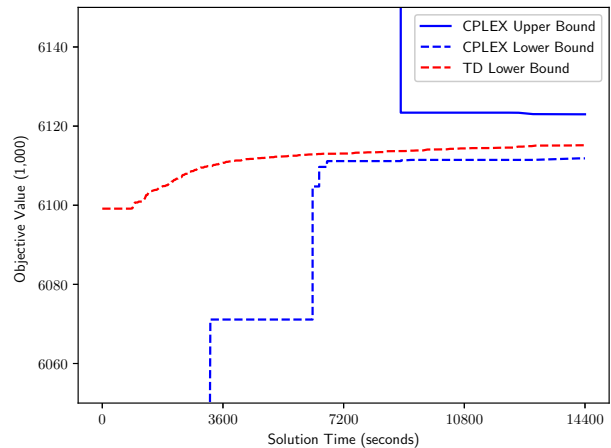


Fig. 7. Progress on the lower and upper bounds for solving the 168-hour unit commitment problem of the PEGASE 1354-bus system by CPLEX and the temporal decomposition TD(24).

the temporal decomposition terminated during the root node solution due to the 4-hour time limit.

V. CONCLUSIONS AND FUTURE WORK

We presented a novel temporal decomposition method that solves a long-term UC problem by splitting the long-term problem into many shorter-term problems based on Lagrangian relaxation, where the shorter-term problems are solved in parallel. We highlight that our decomposition scheme can be applied to other problems such as market and system operations. The computational results on the IEEE 118-bus system showed that the parallel temporal decomposition reduces the solution time by 92% for solving a 96-hour horizon UC problem, which could not be solved to optimality by CPLEX with the 4-hour time limit.

For the IEEE 118-bus system, we not only reported the optimality gaps of the UC solutions but also found that suboptimal generator schedules (even with small optimality gap) can deviate significantly from an optimal schedule. We also showed that even optimal schedules can accumulate a large estimation error, when smaller time windows are used in the rolling horizon approach. Moreover, the rolling horizon approach was not necessarily faster than the temporal decomposition applied to the full planning horizon. The computational results on the IEEE 118-bus system illustrate that the improvement in solution quality and time can lead to higher fidelity PCM simulations.

For the PEGASE 1354-bus system case, we have identified that the master problem solution becomes a computational bottleneck of the temporal decomposition method because of the increasing number of generators and thus coupling constraints. We are currently developing the parallelization of the master solutions based on the ideas in [25], [26] for mitigating the computational bottleneck in the master solution. In particular, we are integrating the parallel interior point solver [27] that implements parallel Schur complement computation for the block-angular structure of the temporal

decomposition master problem. We also plan to develop and integrate primal methods (e.g., cutting planes and heuristics) in the temporal decomposition, which would accelerate the solution.

ACKNOWLEDGMENT

This material is based upon work supported by the U.S. Department of Energy, Office of Electricity Delivery & Energy Reliability/Office of Energy Efficiency & Renewable Energy, under contract number DE-AC02-06CH11357. We gratefully acknowledge the computing resources provided on Blues, a high-performance computing cluster operated by the Laboratory Computing Resource Center at Argonne National Laboratory. The authors thank anonymous reviewers for their constructive comments. The first author also thanks Christian Tjandraatmadja for his contributions to the earlier version of the algorithm implementation.

REFERENCES

- [1] A. Bloom, A. Townsend, D. Palchak, J. King, E. Ibanez, C. Barrows, M. Hummon, and C. Draxl, "Eastern renewable generation integration study," National Renewable Energy Laboratory, Tech. Rep. NREL/TP-6A20-64472, 2016.
- [2] REN21, *Renewables 2016: Global Status Report*. Renewable Energy Policy Network for the 21st Century (REN21), 2016.
- [3] H. Farhangi, "The path of the smart grid," *IEEE Power and Energy magazine*, vol. 8, no. 1, 2010.
- [4] A. Botterud, Z. Zhou, J. Wang, J. Sumaili, H. Keko, J. Mendes, R. J. Bessa, and V. Miranda, "Demand dispatch and probabilistic wind power forecasting in unit commitment and economic dispatch: A case study of illinois," *IEEE Transactions on Sustainable Energy*, vol. 4, no. 1, pp. 250–261, 2013.
- [5] C. Barrows, M. Hummon, W. Jones, and E. Hale, "Time domain partitioning of electricity production cost simulations," National Renewable Energy Laboratory, Tech. Rep. NREL/TP-6A20-60969, January 2015.
- [6] H. Ma and S. Shahidehpour, "Transmission-constrained unit commitment based on Benders decomposition," *International Journal of Electrical Power & Energy Systems*, vol. 20, no. 4, pp. 287–294, 1998.
- [7] Y. Fu, M. Shahidehpour, and Z. Li, "Long-term security-constrained unit commitment: hybrid dantzig-wolfe decomposition and subgradient approach," *IEEE Transactions on Power Systems*, vol. 20, no. 4, pp. 2093–2106, 2005.
- [8] M. A. Bragin, P. B. Luh, J. H. Yan, N. Yu, and G. A. Stern, "Convergence of the surrogate lagrangian relaxation method," *Journal of Optimization Theory and applications*, vol. 164, no. 1, pp. 173–201, 2015.
- [9] K. Kim and V. M. Zavala, "Large-scale stochastic mixed-integer programming algorithms for power generation scheduling," in *Alternative Energy Sources and Technologies*. Springer, 2016, pp. 493–512.
- [10] —, "Algorithmic innovations and software for the dual decomposition method applied to stochastic mixed-integer programs," *Mathematical Programming Computation (to appear)*, 2017.
- [11] N. P. Padhy, "Unit commitment—a bibliographical survey," *IEEE Transactions on Power Systems*, vol. 19, no. 2, pp. 1196–1205, 2004.
- [12] Z. Zhou, C. Liu, and A. Botterud, "Stochastic methods applied to power system operations with renewable energy: A review," Argonne National Laboratory, Tech. Rep. ANL/ESD-16/14, 2016.
- [13] J. A. Muckstadt and S. A. Koenig, "An application of Lagrangian relaxation to scheduling in power-generation systems," *Operations Research*, vol. 25, no. 3, pp. 387–403, 1977.
- [14] W. L. Peterson and S. R. Brammer, "A capacity based Lagrangian relaxation unit commitment with ramp rate constraints," *IEEE Transactions on Power Systems*, vol. 10, no. 2, pp. 1077–1084, 1995.
- [15] T. Li and M. Shahidehpour, "Price-based unit commitment: A case of lagrangian relaxation versus mixed integer programming," *IEEE transactions on power systems*, vol. 20, no. 4, pp. 2015–2025, 2005.
- [16] N. J. Redondo and A. Conejo, "Short-term hydro-thermal coordination by Lagrangian relaxation: solution of the dual problem," *IEEE Transactions on Power Systems*, vol. 14, no. 1, pp. 89–95, 1999.
- [17] G. B. Dantzig and P. Wolfe, "Decomposition principle for linear programs," *Operations Research*, vol. 8, no. 1, pp. 101–111, 1960.
- [18] J. Ostrowski, M. F. Anjos, and A. Vannelli, "Tight mixed integer linear programming formulations for the unit commitment problem," *IEEE Transactions on Power Systems*, vol. 27, no. 1, pp. 39–46, 2012.
- [19] S. Atakan, G. Lulli, and S. Sen, "A state transition mip formulation for the unit commitment problem," *IEEE Transactions on Power Systems*, 2017.
- [20] K. C. Kiwiel, "Proximity control in bundle methods for convex nondifferentiable minimization," *Mathematical Programming*, vol. 46, no. 1, pp. 105–122, 1990.
- [21] Y. Xu, T. K. Ralphs, L. Ladányi, and M. J. Saltzman, "Alps: A framework for implementing parallel tree search algorithms," in *The Next Wave in Computing, Optimization, and Decision Technologies*. Springer, 2005, pp. 319–334.
- [22] "PJM - Estimated Hourly Load," <http://www.pjm.com/markets-and-operations/energy/real-time/load/hr.aspx>, accessed: 2017-04-26.
- [23] J. N. Puga, "The importance of combined cycle generating plants in integrating large levels of wind power generation," *The Electricity Journal*, vol. 23, no. 7, pp. 33–44, 2010.
- [24] S. Fliscounakis, P. Panciatici, F. Capitanescu, and L. Wehenkel, "Contingency ranking with respect to overloads in very large power systems taking into account uncertainty, preventive, and corrective actions," *IEEE Transactions on Power Systems*, vol. 28, no. 4, pp. 4909–4917, 2013.
- [25] M. Lubin, K. Martin, C. G. Petra, and B. Sandıkçı, "On parallelizing dual decomposition in stochastic integer programming," *Operations Research Letters*, vol. 41, no. 3, pp. 252–258, 2013.
- [26] B. Dandurand and K. Kim, "Scalable decomposition methods for preventive security-constrained optimal power flow," Argonne National Laboratory, Tech. Rep. ANL/MCS-P9021-1117, 2017.
- [27] C. G. Petra, O. Schenk, M. Lubin, and K. Gärtner, "An augmented incomplete factorization approach for computing the schur complement in stochastic optimization," *SIAM Journal on Scientific Computing*, vol. 36, no. 2, pp. C139–C162, 2014.